Clays Clay Miner. (2023) 71:637–649
https://doi.org/10.1007/s42860-023-00265-1

ORIGINAL PAPER

A New Preparation Method for *cis*-1,4-polyisoprene/Na-montmorillonite Latex Composites by in situ Solution Emulsification

Liyun Guo · Haichang Zhang · Jing Hua · Danfeng Liu

Accepted: 21 November 2023 / Published online: 12 December 2023

Abstract *Cis*-1,4-polyisoprene latex (IRL) is the best alternative to natural rubber latex (NRL), and can help to avoid human allergic reactions caused by proteins in NRL. The mechanical properties of IRL are inferior to those of NRL, however. To address this issue, a novel strategy was developed using an in situ solution emulsification to prepare a latex composite incorporating sodium montmorillonite (Na-Mnt). The properties of the latex film prepared were investigated. The dispersion state of the Mnt in the latex composites and the morphology of the resulting composite films were characterized using scanning electron microscopy (SEM) and transmission electron microscopy (TEM). In addition, the mechanism of Mnt reinforcement of IRL is described comprehensively. The results showed that the Mnt/IRL latex composites prepared were stable and excellent films were formed, similar to those of NRL. The current research provided an effective method for preparing high-performance composite films suitable for use in high-end medical applications.

Keywords Artificial latex · *Cis*-1,4-polyisoprene rubber latex (IRL) · Hybrid/latex composites · In situ solution emulsification · Na montmorillonite (Na-Mnt)

Associate Editor: Georgios D. Chryssikos

L. Guo · H. Zhang · J. Hua (✉) · D. Liu
Key Laboratory of Rubber-Plastics, Ministry of Education, College of Polymer Science and Engineering, Qingdao University of Science and Technology, Qingdao 266042, China
e-mail: huajing72@qust.edu.cn

Introduction

In 2020, COVID-19 spread all over the world and resulted in a shortage of medical and health latex products. The main raw material for latex products is natural rubber latex (NRL), which is mainly composed of *cis*-1,4-polyisoprene. NRL is abstracted from *Hevea brasiliensis (Willd. ex A. Juss.) Muell. Arg.*, which has excellent properties such as biocompatibility, good mechanical properties, and good film-forming performance. However, NRL can easily cause allergic reactions in humans because it contains at least 14 proteins (Hev b1-14). NRL is not suitable for latex products that are to be used in contact with the skin (Nielsen et al., 2007). Searching for non-allergenic materials with good film-forming properties, good biological properties, and low cost has become essential. Similar to *cis*-1,4-polyisoprene latex (IRL), guayule natural rubber (Ren et al., 2020) and dandelion rubber (Tang et al., 2022) have a high safety index for high-end medical healthcare applications because they do not contain protein and would not cause an allergic reaction. However, guayule and dandelion natural rubbers are usually in solid form and cannot be used directly as latex. Using IRL is

one of the most effective ways to solve this problem of allergy, therefore, but only a few studies to date have described its preparation. Because IRL contains no non-rubber components such as protein and phospholipid layers around the latex particles, however, the film-forming property is not as good as that of NRL and the tensile strength is also less. Therefore, strengthening the mechanical properties of the IRL films is essential.

Montmorillonite (Mnt) is a natural clay mineral that is often used to produce clay-polymer nanocomposites. Its large swelling capacity allows it to exfoliate, forming particles with thicknesses in the nanometer range and transverse size in the micrometer range. These particles are classified as nanofillers when dispersed in a polymeric matrix; even at low fill loading, they can change and improve the properties of polymer materials, such as gas permeability resistance, modulus, mechanical strength, thermal stability, and flame retardancy (Dubois & Alexandre, 2000). At present, studies of the preparation and characterization of nitrile-butadiene rubber (NBR)/styrene butadiene rubber (SBR)/Mnt, SBR/Mnt, NR/Mnt, and NBR/Mnt composites and clay polymer nanocomposites have been reported (Archibong et al., 2023; Arroyo et al., 2003; de Oliveira & Beatrice, 2018; Devi et al., 2015; Esmaeili et al., 2021; Essawy & El-Nashar, 2004; Hrachová et al., 2008; Joly et al., 2002; Kader et al., 2006; Khalid et al., 2016; Valadares et al., 2006; Zhang et al., 2005). Note, however, that the direct addition of clay nanoparticles to latex can cause filler precipitation, absorption of stabilizer in latex, an increase in the latex viscosity, destabilization of the latex, and even latex coagulation. Latex products are produced using a latex dipping process and require a stable latex state, so latex coagulation is not expected and undesirable in terms of various production processes. The traditional latex composite technology, known as the latex co-precipitation method or latex blending method, involves mixing a clay-water suspension together with rubber latex and then pouring them into a flocculant solution for flocculation to obtain composite materials. This method destroys the original state of the latex, however, and its composite materials cannot be used in the production of latex products, which limits their utility.

To overcome these shortcomings and address this issue, latex composites of Mnt/IRL were prepared using Mnt as the reinforcing agent during the IRL preparation process. To the present authors' knowledge, few detailed published reports exist on the addition of Mnt to IR latex during the preparation process to obtain Mnt/IRL latex composites. The objective of the present study, therefore, was to evaluate the basic properties of Mnt/IRL composites through measurements of total solid content, particle size, and zeta potential, and then to investigate the effect of the amount of Mnt on the resulting latex film properties and their dispersion states. The hypothesis was that integrating the two steps of emulsification and reinforcement modification into a single process would not only simplify production, but would also ensure the dispersion of Mnt.

Experimental

Materials

Na-Mnt, sample K10 from Southern Clay Products (Gonzales, Texas, USA), with a cation exchange capacity (CEC) of 102 meq/100 g of clay and specific surface area of 240 m^2/g was used. *Cis*-1,4-polyisoprene rubber (IR2200) was obtained from Zeon Corporation (Tokyo, Japan). NRL with 50% solid content was provided by the 11th Rubber Plant of Guangzhou, China. Cyclohexane, sodium lauryl sulfonate (SLS, as the main emulsifier), potassium oleate (as the co-emulsifier), sulfur (as the curing agent), zinc oxide (ZnO as the activator), zinc diethyldithiocarbamate (ZDC as the accelerator), N-isopropyl-N'-phenyl-p-phenylenediamine (4010NA as the antioxidant), potassium hydroxide (KOH as pH regulator), and casein (as stabilizer) were of industrial grade and were obtained from Sinopharm Chemical Reagent Co., Ltd (Shanghai, China). Distilled water was used throughout the experiments. All the experimental materials were used as received.

Preparation of Latex Composites

First, IR rubber solution (10 wt.% IR rubber solution in cyclohexane, oil phase) was prepared using a mechanical stirrer at a speed of 200–300 rpm in cyclohexane for 6 h at room temperature. An emulsifier solution of SLS and potassium oleate (aqueous phase: SLS, 1.5 wt.%; potassium oleate, 0.5 wt.%) was also prepared using a

https://doi.org/10.1007/s42860-023-00265-1 Published online by Cambridge University Press

mechanical stirrer at a speed of 200–300 rpm in distilled water for 2 h at 45 ℃. A 50 wt.% slurry of Mnt in distilled water was prepared. Then the Mnt suspension was added to the oil phase and blended mechanically under strong shear force.

Secondly, various amounts of Mnt suspension (0, 1, 3, 4, and 5 phr, phr: parts per hundred of rubber) were added to an IR rubber cyclohexane solution and stirred mechanically at 300 rpm for 15 min. The amounts of Mnt were calculated on an IR mass basis. The Mnt-modified oil phase was obtained.

Third, the Mnt-modified oil phase was added to the aqueous phase for emulsification at a high speed (6000 rpm) for 30 min. After solvent recovery and centrifugal concentration processes, the latex composites with various amounts of Mnt (0, 1, 3, 4, and 5 phr) were obtained. The corresponding latex composites were named IRL, Mnt/IRL (1 phr), Mnt/IRL (3 phr), Mnt/IRL (4 phr), and Mnt/IRL (5 phr), respectively.

Preparation of the Composite Films

For preparation of the films, aqueous dispersions of ZnO (50%), ZDC (50%), 4010NA (50%), and sulfur (50%) were mixed in a planetary ball mill with the required amount of water and with the aid of casein stabilizer. Then the compounded latexes were prepared by mixing the IRL, Mnt/IRL (1 phr), Mnt/IRL (3 phr), Mnt/IRL (4 phr), and Mnt/IRL (5 phr) with the aqueous dispersion containing ZnO (50%), ZDC (50%), 4010NA (50%), sulfur (50%), and 10% KOH, and stirring for 30 min using a mechanical stirrer at a speed of 200–300 rpm. The compounded latex was then heated to 60°C in a water bath for 10 h to pre-vulcanize it. The formula for the compounded latex used was as follows: IR 100 phr, ZnO 2 phr, sulfur 1 phr, 4010 NA 1 phr, ZDC 1.5 phr, and KOH 0.3 phr. The pre-vulcanized latexes were then left to mature for>24 h without stirring to promote the diffusion of chemical additives, which ensured the uniform properties of the latex

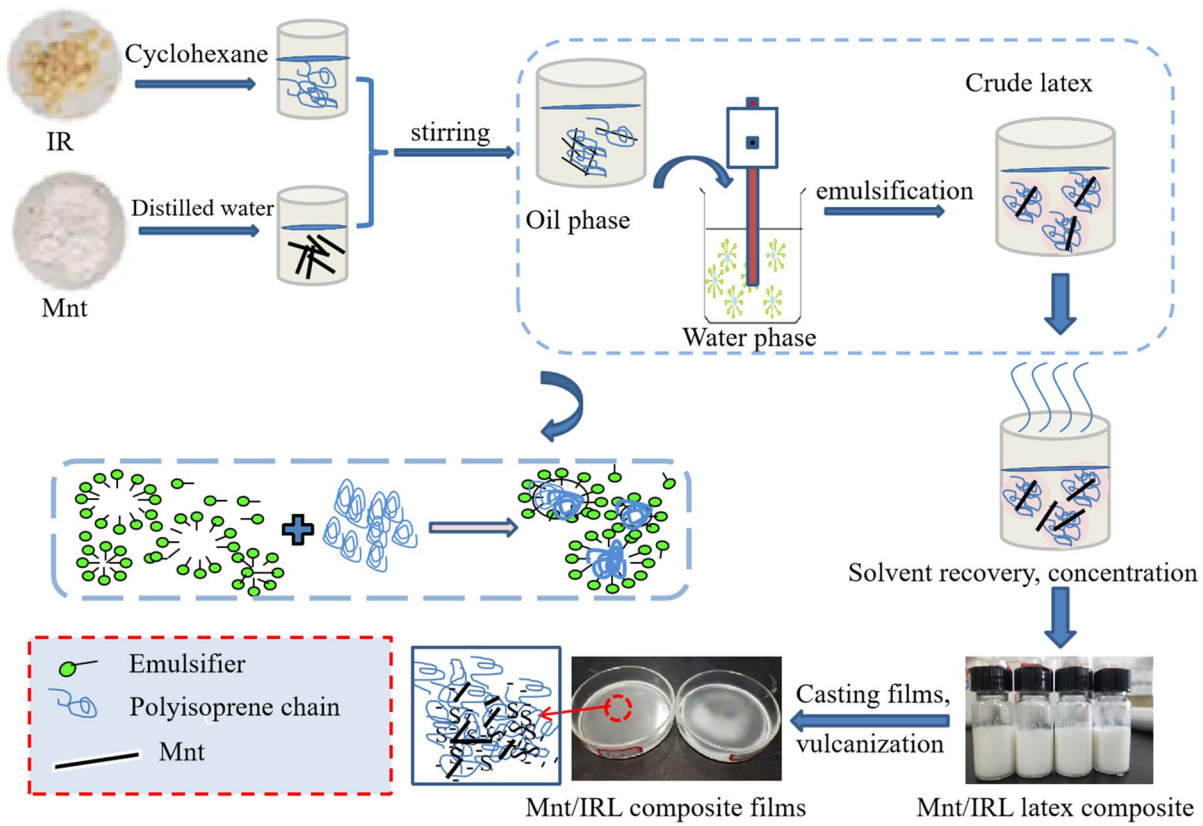

Fig. 1 Schematic diagram of the preparation processes for IRL and Mnt/IRL latex composites

https://doi.org/10.1007/s42860-023-00265-1 Published online by Cambridge University Press

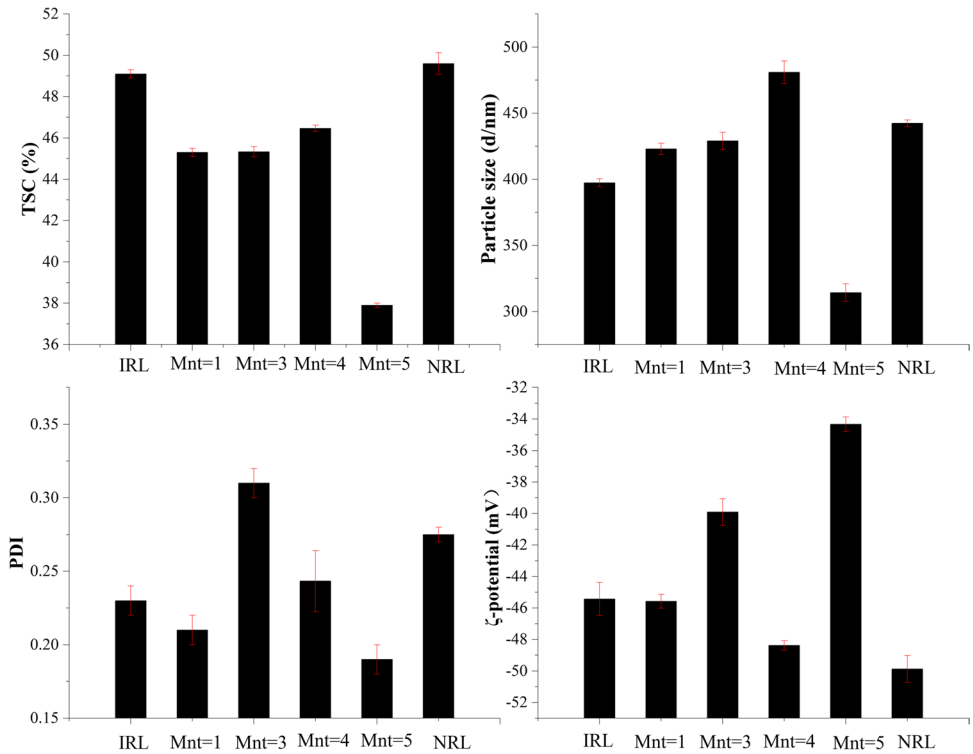

Fig. 2 The TSC, particle size, PDI, and ζ-potential of IRL and Mnt/IRL latex composites: Columns from left to right are IRL, Mnt/IRL (1 phr), Mnt/IRL (3 phr), Mnt/IRL (4 phr), Mnt/IRL (5 phr), NRL

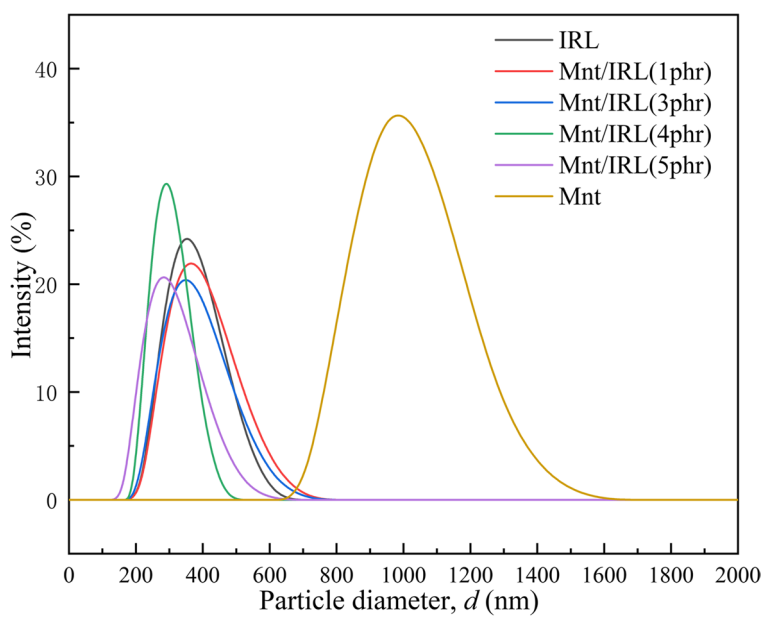

Fig. 3 The particle-size distribution index of the IRL, Mnt, and Mnt/IRL latex composites

https://doi.org/10.1007/s42860-023-00265-1 Published online by Cambridge University Press

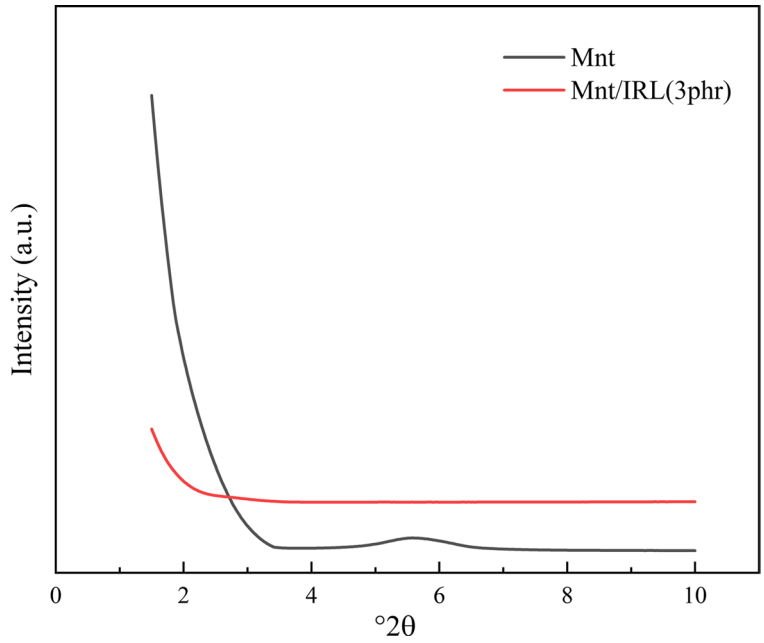

Fig. 4 XRD patterns of the Mnt and Mnt/IRL (3 phr) composite films

films. They were filtered through a sieve (300 mesh filter screen with a pore size of 48 μm). Finally, they were cast on a petri dish with a diameter of 80 mm and spread the latex evenly on the surface. The latexes were allowed to dry in the air until they became transparent and then were vulcanized in the oven at 100°C for 30 min. Before testing, the vulcanized rubber films were stored in a desiccator. A schematic diagram of process of preparing the IRL and Mnt/IRL latex composites is shown in Fig. 1.

Characterization

Total Solid Content (TSC)

The latex was weighed accurately (0.200 ± 0.001 g, W_0) and placed on a watch glass (diameter of 60 mm), then heated in a hot-air oven at 70 ± 2°C until a constant weight was achieved. The dried sample was removed from the oven and cooled to room temperature in a desiccator. The films were peeled off the watch glass and weighed, giving W_{TSC}. The TSC was calculated using Eq. 1. Three replicates were measured.

$$TSC = W_{TSC}/W_0 \times 100\% \quad (1)$$

Particle Size and ζ-potential

The particle size, size distribution index (PI), and ζ-potential of Mnt and all the latex composites were measured by ZetaPALS (Brookhaven Instruments, New York, USA) at 25 ± 2°C. Before measurement, the latex samples were diluted 100 times with distilled water. Three replicates were measured.

X-ray Diffraction (XRD)

XRD analysis of the Mnt and Mnt/IRL (3 phr) latex composite films was performed using a diffractometer (Bruker D8 Discover, Massachusetts, USA) equipped with Lynx Eye and Vantec-500 detectors and operating at 40 kV and 40 mA with CuKα radiation (1.5418 Å). Mnt was measured in powder form. The experimental conditions had an angle range of 1.5–10°2θ, the scan rate was 1.2°2θ per min, and the step size was 0.02°2θ.

Transmission Electron Microscopy (TEM)

All the IRL latex samples were imaged using a JEM2100 transmission electron microscopy (JEOL,

https://doi.org/10.1007/s42860-023-00265-1 Published online by Cambridge University Press

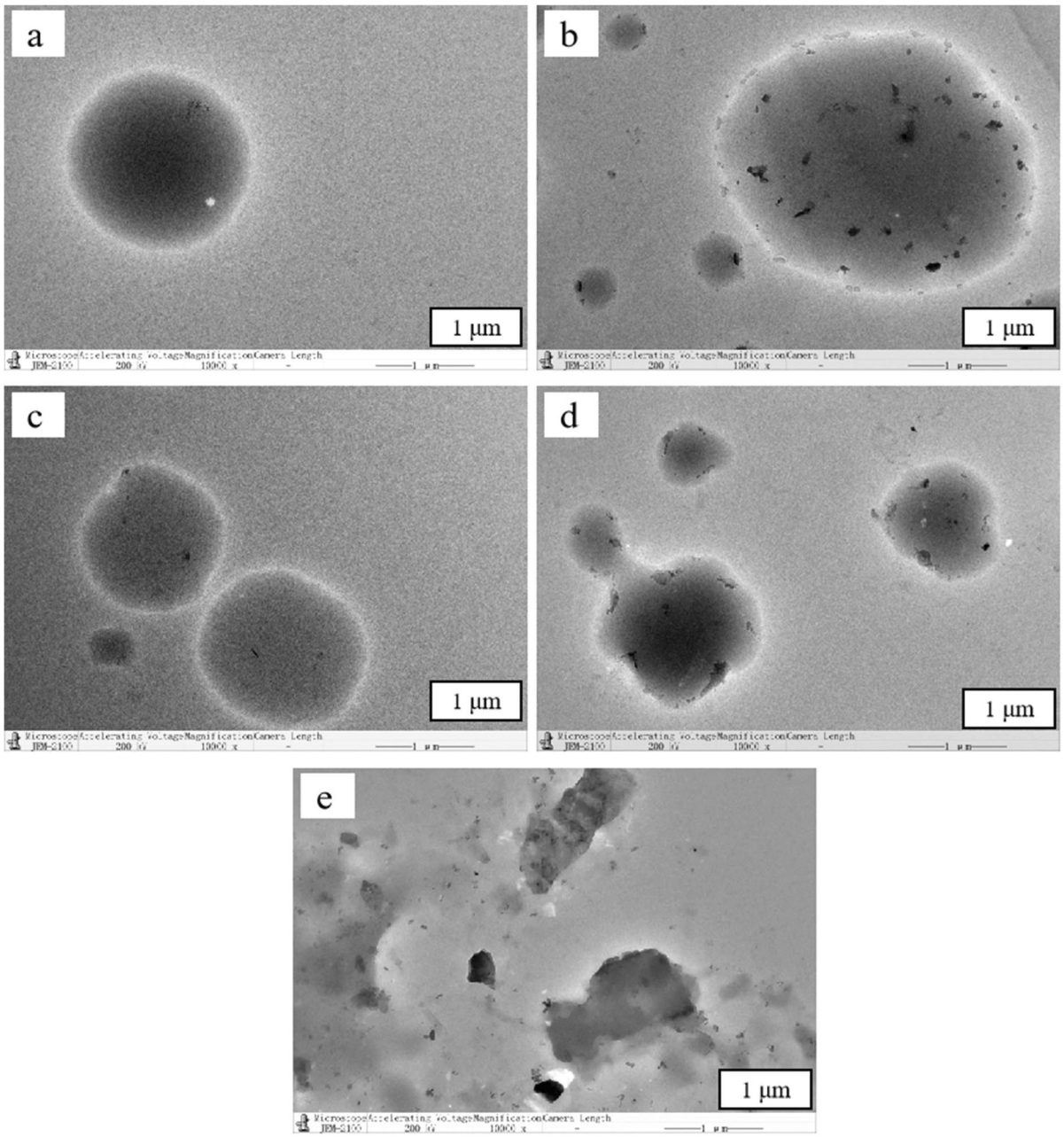

Fig. 5 TEM images of Mnt/IRL latex composites: **a** IRL, **b** Mnt/IRL (1 phr), **c** Mnt/IRL (3 phr), **d** Mnt/IRL (4 phr), and **e** Mnt/IRL (5 phr)

Tokyo, Japan) operated with an accelerating voltage of 200 kV. Before examination, the TEM samples were prepared by depositing the latex dispersion in deionized water onto a copper grid covered with a carbon film.

Scanning Electron Microscopy (SEM)

SEM images were acquired using a high-resolution scanning microscopy of JSM7500F (JEOL, Tokyo, Japan) at 2 kV. The take-off angle was 35°. The IRL film and the Mnt-IRL composite films were fractured

https://doi.org/10.1007/s42860-023-00265-1 Published online by Cambridge University Press

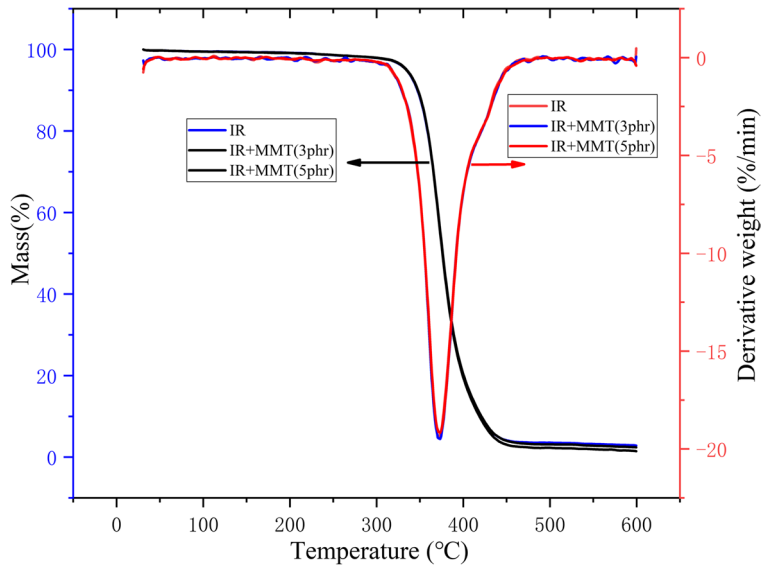

Fig. 6 TGA and DTGA analysis of IRL and Mnt/IRL composite films

cryogenically in liquid nitrogen before examination. The film samples were placed flat on the SEM stub using double-sided tape. The films were sputter-coated for 3 min under a vacuum with a thin layer of gold before observation.

Thermogravimetric Analysis (TGA)

A Shimadzu DTG-60H thermogravimetric analyzer (TGA) (Kyoto, Japan) was used to investigate the thermal stability of IRL, IRL/Mnt(3 phr), and IRL/Mnt(5 phr) films. A 5–8 mg sample was weighed and placed on an aluminum plate. The experiments were conducted under N_2 flow (50 mL min^{-1}), from 30 to 550°C with a heating rate of 10°C min^{-1}.

Mechanical Properties

The tensile strength test was carried out using a GT-AI-7000S electronic tensile machine produced by GOTECH Testing Machines Inc (Dongguan, China) using dumb-bell-shaped test specimens at a temperature of 23 ± 2°C for all the film samples, in accordance with the ASTM D 412 standard. The tensile strain rate was 500 mm/min.

Results and Discussion

Characterization of Mnt/IRL Latex Composites

The particle size and its distribution index, the TSC, and the ζ-potential of the latex composites were determined as a function of increasing Mnt content (Figs. 2 and 3). When the amount of Mnt was <5 phr, the TSC of the latex was high because the ζ-potential of Mnt was –20.9 mV. Negatively charged Mnt repels the negatively charged polyisoprene latex particles and promotes the stability of latex. When the ζ-potential values were > ± 30 mV, the physical stability of the colloidal systems is good, which indicates a long shelf life (Riddick, 1968). As in Fig. 2, the surface charge of IRL had a negative value of > ± 30 mV. Thus, IRL and Mnt/IRL latex composites are expected to be stable when stored at ambient temperatures.

Compared to the particle size of the neat IRL, the mean particle size of the Mnt/IRL composite increased from ~420 to 475 nm as the amount of Mnt increased from 1 to 4 phr. However, when the amount of Mnt added increased to 5 phr, the particle size and TSC decreased. This is mainly attributed to agglomeration of the excess Mnt, which

https://doi.org/10.1007/s42860-023-00265-1 Published online by Cambridge University Press

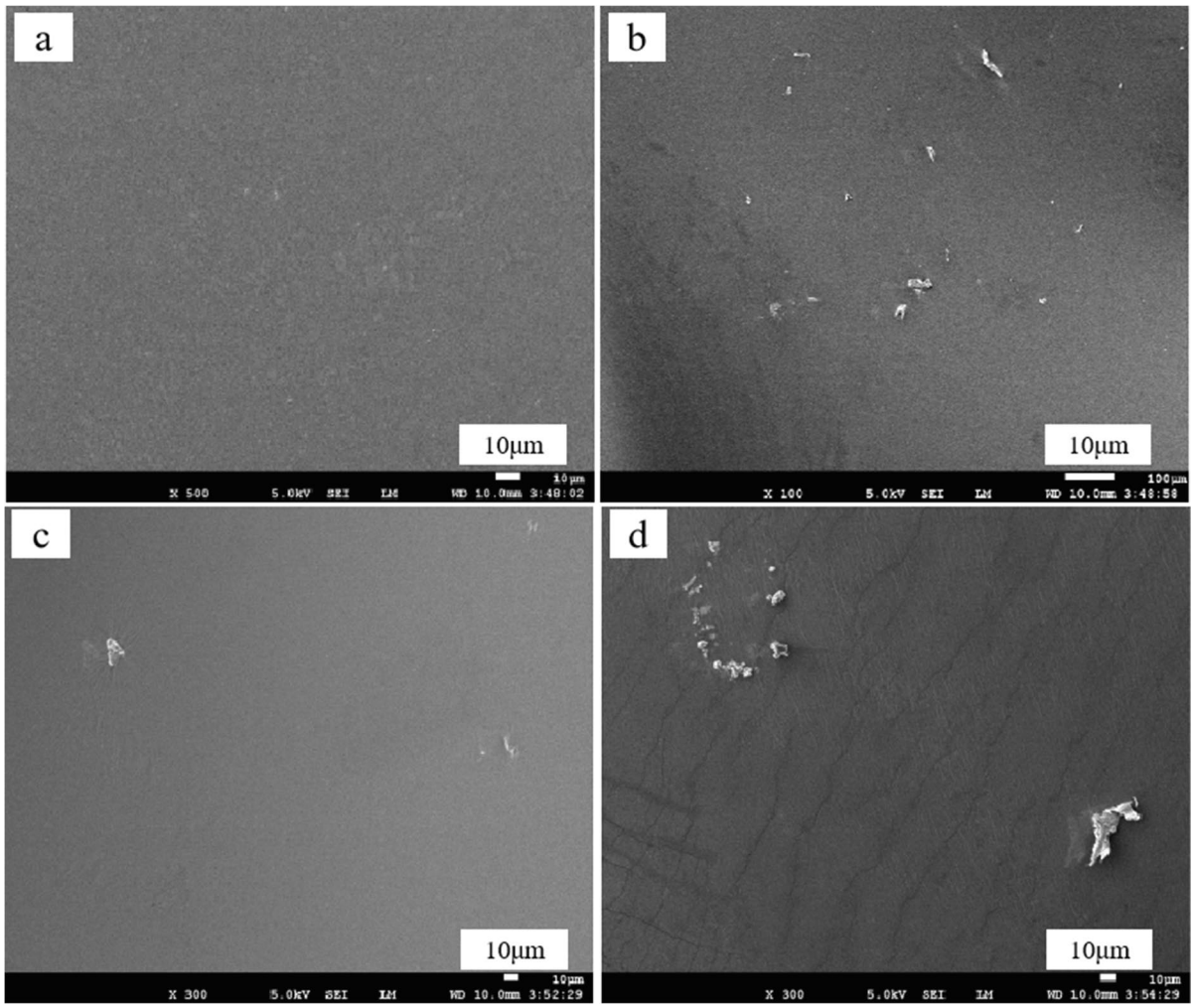

Fig. 7 SEM images of the IRL and Mnt/IRL composite films surface: **a** IRL, **b** Mnt/IRL (1 phr), **c** Mnt/IRL (3 phr), and **d** Mnt/IRL (5 phr)

destroys the stability of the latex state. Furthermore, all the IRL composites had a single peak and a low PDI, indicating that the particles had a relatively narrow size distribution (Fig. 3). The particle size of all latex composites was smaller than that of Mnt (~1 μm), which is due to the strong shear during the emulsification process, resulting in a significant reduction in the Mnt particle size.

Compared to NRL, the above results indicated that when the amount of Mnt was <5 phr, all the as-prepared Mnt/IRL composites were stable, had a large solids content and small particle sizes, similar to the performance of NRL.

XRD of the Mnt and Mnt/IRL Composite Films

Mnt has characteristic diffraction peaks corresponding to its ordered silicate layers in the XRD patterns of the Mnt and Mnt/IRL composite films (Fig. 4). The peak intensity at 5.73°2θ corresponds to the reflection of the (001) planes of Mnt. The absence of a 001 reflection in the patterns of the composite films indicates that Mnt is present as exfoliated layers and a uniform structure is formed between Mnt and IR rubber macromolecular chains.

https://doi.org/10.1007/s42860-023-00265-1 Published online by Cambridge University Press

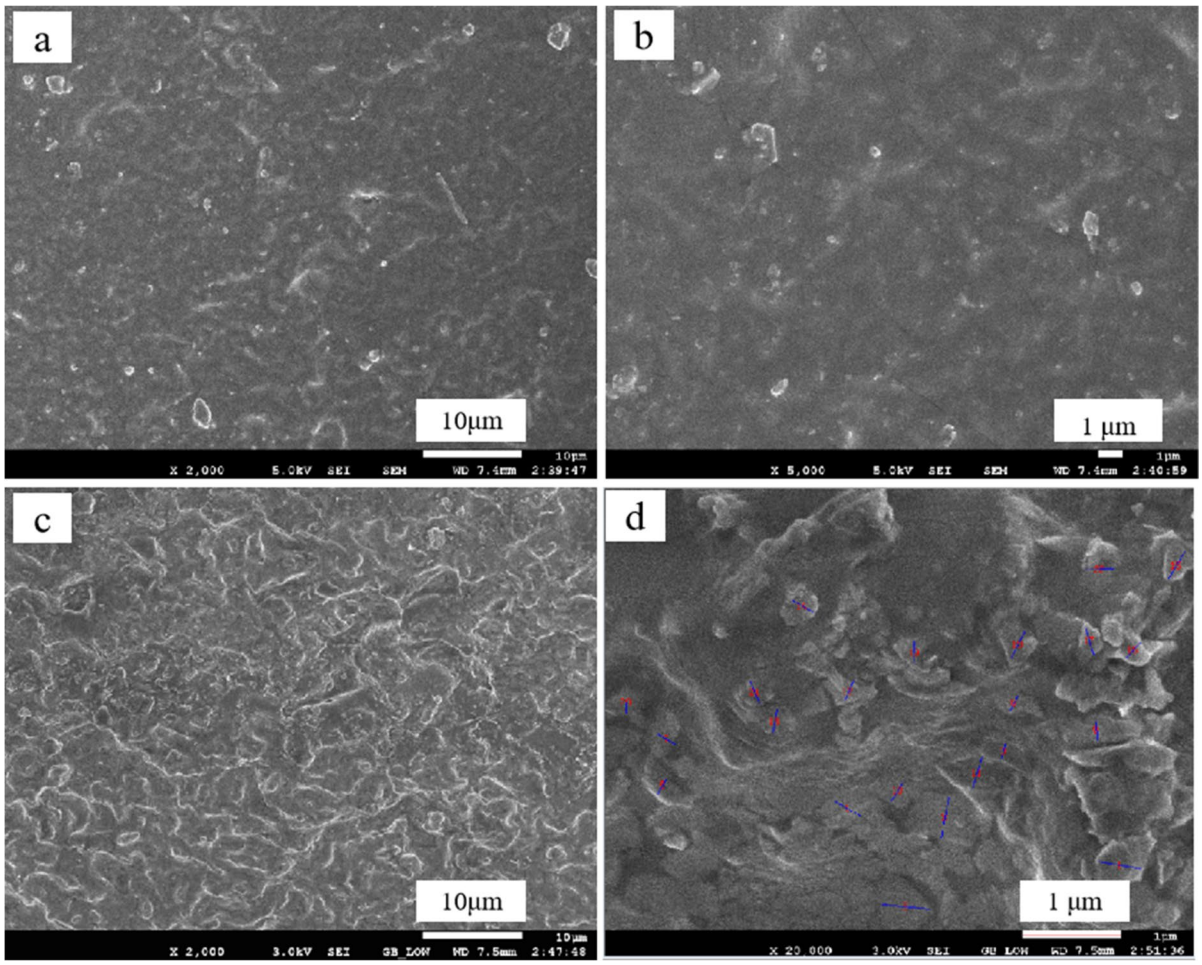

Fig. 8 SEM images of the fractured IRL and Mnt/IRL composite vulcanized films: **a**, **b** IRL and **c**, **d** Mnt/IRL (1 phr)

Morphology of the Mnt/IRL Latex Composites

The TEM images of the IRL and Mnt/IRL latex composites containing 0, 1, 3, 4, and 5 phr Mnt (Fig. 5) showed that when the amount of Mnt was 0 phr, the latex particles were spherical. With the addition of increasing amounts of Mnt, aggregated Mnt on the surface of the latex particles was observed. The best dispersion was observed when the amount of Mnt was 3 phr. At 4 phr Mnt, the latex particles began to aggregate to a significant extent. As the amount of Mnt increased to 5 phr, agglomeration occurred in the Mnt/IRL latex composites, and the spherical structure of the original latex particles was destroyed (Fig. 5e), which was consistent with the test results regarding particle size. The optimal amount of Mnt was 3 phr.

Thermogravimetric Analysis (TGA) of the IRL and Mnt/IRL Composite Films

The TGA and DTGA curves for IRL and Mnt/IRL composite films containing 3 and 5 phr Mnt (Fig. 6) revealed initial degradation of the films at ~334℃; the maximum degradation occurred at 373°C, which was the same as pristine IR. Mnt does not increase the thermal stability of the Mnt/IRL composite films.

SEM of IRL and Mnt/IRL Composite Films

SEM of Raw Rubber Composite Films

Characterization of the morphology of the raw rubber film surface is shown in Fig. 7. The film

https://doi.org/10.1007/s42860-023-00265-1 Published online by Cambridge University Press

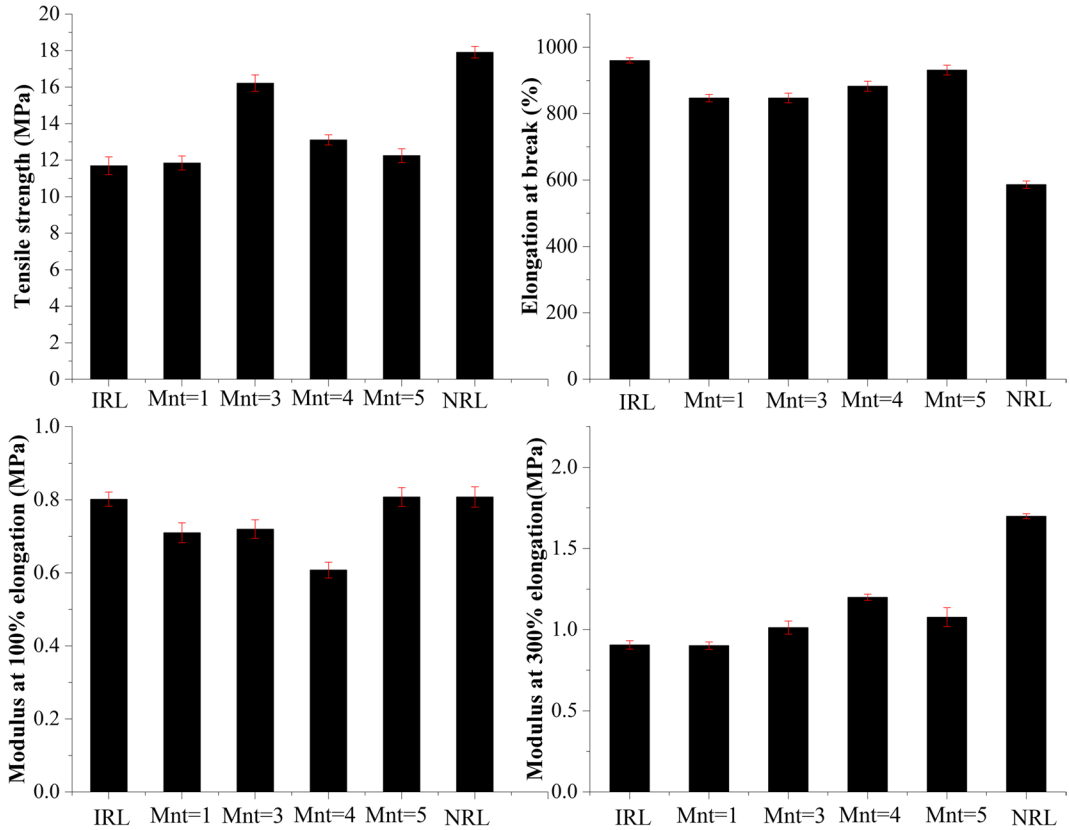

Fig. 9 Mechanical properties of the IRL and Mnt/IRL composite films: Columns from left to right are IRL, Mnt/IRL (1 phr), Mnt/IRL (3 phr), Mnt/IRL (4 phr), Mnt/IRL (5 phr), NRL

samples were prepared by the casting method. The latexes were cast on a petri dish (diameter = 80 mm) and left to dry in air until transparent. This showed that the pure IRL films had a flat and smooth surface. When the amount of Mnt was ≤3 phr, there was little change to the surface, indicating good compatibility between the IR macromolecules and Mnt. However, when the amount of Mnt increased to 5 phr, significant aggregation of Mnt particles occurred and cracks appeared in the film surface. This occurred because Mnt particles, serving as dispersed phases, aggregated and formed stress concentration points in the film. Due to the rigidity of the Mnt particles, they did not deform under stress, leading to cracks on the surface of the film and a decrease in its strength. Therefore, when the amount of Mnt was 3 phr, the composite films had the best surface appearance.

SEM of the Fractured Surface of IRL and Mnt/IRL Vulcanized Composite Films

The morphology of the fractured Mnt/IRL vulcanized composite films is shown in Fig. 8. The interface between filler and rubber matrix was investigated by observing the quenched section of the Mnt/IRL films. The cross-section of the pure IRL film was relatively flat, which indicated that the system was homogeneous. However, the vulcanized film with 3 phr Mnt had a rough and reticular section with obvious tensile filaments and a pulled Mnt lamellar structure, which indicated that Mnt enhanced the interfacial interaction between IR macromolecules and Mnt layers and increased the mechanical properties of the rubber film (Hu et al., 2020). Mnt was well dispersed in the IR matrix and clusters and blocks of uneven size were not

https://doi.org/10.1007/s42860-023-00265-1 Published online by Cambridge University Press

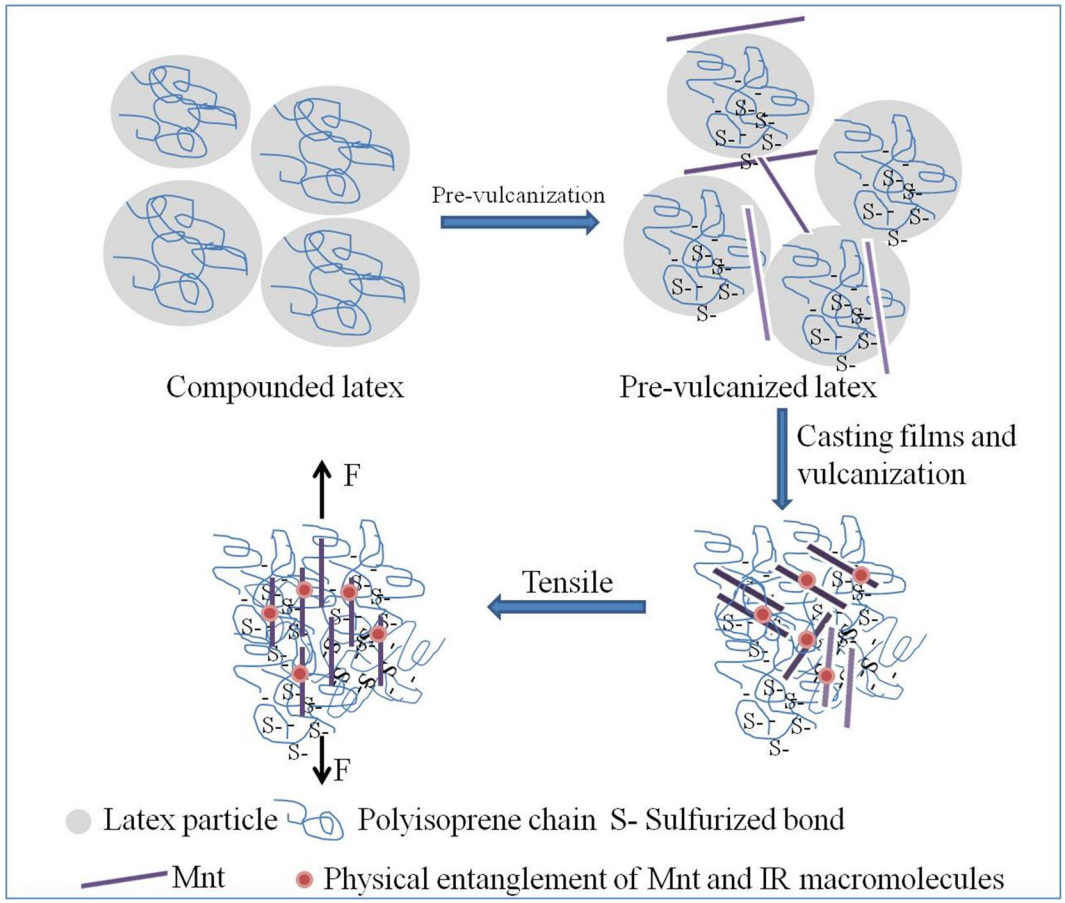

Fig. 10 Vulcanization mechanism and structure scheme of Mnt/IRL composite films

observed (Fig. 8c), even at higher magnification. Mnt was observed to be uniformly dispersed and wrapped in the IR macromolecules (Fig. 8d).

Mechanical Properties of the IRL and Mnt/IRL Composite Films

The measured mechanical properties of the vulcanized films of pure IRL and Mnt/IRL composite films with various amounts of Mnt (Fig. 9) revealed that, when the amount of Mnt was < 5 phr, the tensile strength and modulus at 300% elongation (M300) of the Mnt/IRL latex composites films were greater than those of the IRL film. With increase in the amount of Mnt, the tensile strength of the Mnt/IRL films increased and reached a maximum value of 16.5 MPa at 3 phr, a 1.4 × greater tensile strength value than those of pure IRL films, i.e. close to the strength of the pure NRL film. This indicates that a small addition of Mnt improves the tensile strength of the IRL films. The improvement in tensile strength of the nano-filler at low additions is mainly due to the strong interfacial interactions between the nano-filler and the rubber matrix, which leads to the uniform dispersion of nano-filler in rubber (Chen et al., 2019; Song et al., 2017; Sui et al., 2008). Above 3 phr Mnt, the tensile strength of the Mnt/IRL films decreased but remained higher than that of the pure IRL film. At high levels of Mnt, the tensile strength of the films decreased, possibly due to the aggregation of Mnt in the polyisoprene rubber matrix.

With increasing amounts of Mnt, the flexibility of polyisoprene macromolecular chains becomes limited and the elongation at break first decreases and then increases. The initial decrease in elongation at break is typically

https://doi.org/10.1007/s42860-023-00265-1 Published online by Cambridge University Press

observed in polymer composites because the Mnt has large rigidity, large specific surface area, and a large aspect ratio, which helps to improve the stiffness and restrict the movement of the rubber chains (Jiang et al., 2015; Rajaraman et al., 2015). Moreover, under high loads, the filler–filler interaction reduces the elongation at break and leads to a reduction in flexibility (Ravindren et al., 2018). The tendency for the elongation at break to increase with increasing amounts of Mnt is due to local Mnt agglomeration, which renders it unable to restrict the movement of the rubber macromolecular chain.

Vulcanization and Reinforcement Mechanism of the Mnt/IRL Composite Films

The aforementioned physical and mechanical properties can be explained from the perspective of Mnt dispersion in latex and the vulcanization mechanism of the rubber film, as illustrated in Fig. 10. During the latex mixing stage, the particles of IRL are mixed with the Mnt aqueous suspension comprising delaminated silicate layers. Each latex particle consists of several rubber macromolecules; these latex particles adsorb onto the already delaminated Mnt layers, resulting in a uniform dispersion of Mnt in the latex. After the drying and film-forming process, the IR rubber macromolecules enter the Mnt layers to form a Mnt/IRL composite film with a uniform dispersion of Mnt. The nanoscale dispersion of Mnt in the IR matrix results in strong binding forces between them and increases crosslinking density in the Mnt/IRL film. In addition, the presence of Mnt layers restricts the movement of the IR macromolecules during stress. This restriction enhances the overall rigidity of the macromolecular chains, leading to a decrease in elongation at break, an increase in tensile strength, and a decrease in the tendency for the growth of cracks.

Consequently, the tensile strength of the Mnt/IRL composite film is enhanced after adding a small amount of Mnt. However, when the amount of Mnt exceeds a certain value, the tensile strength of the composite decreases due to Mnt agglomeration, resulting in poor compatibility between Mnt and the IR matrix.

Conclusions

In summary, Mnt/IRL was prepared using in situ solution emulsification. Stable Mnt/IRL latex composites with large solid content, small particle size, and excellent film formation was achieved. The XRD patterns and TEM images showed good dispersion of Mnt in the Mnt/IRL latex composites. The results of the SEM and mechanical-properties tests showed that Mnt was dispersed uniformly and wrapped among the polyisoprene macromolecules at the nanometer level, which enhanced significantly the interaction between Mnt and rubber macromolecular chains and greatly improved the physical and mechanical properties. When the amount of Mnt was 3 phr, the distribution of Mnt in the latex was most uniform, and the resulting composite film had a smooth appearance, and mechanical properties were similar to those of NRL films. Compared to the IRL films, the tensile strength of Mnt/IRL (3 phr) composite film increased by 39.8%. These results provide a novel method for designing and preparing composite films with good mechanical properties.

Acknowledgements This study was supported financially by the Natural Science Foundation of Shandong Province (ZR2020ME059 and ZR2021ME028).

Data Availability All data generated or analysed during this study are included in this published article [and its supplementary information files].

Declarations

Conflict of Interest The authors declare that they have no conflict of interest.

References

Archibong, F. N., Orakwe, L. C., Ogah, O. A., Mbam, S. O., Ajah, S. A., Okechukwu, M. E., Igberi, C. O., Okafor, K. J., Chima, M. O., & Ikelle, I. I. (2023). Emerging progress in montmorillonite rubber/polymer nanocomposites: A review. *Journal of Materials Science, 58*(6), 2396–2429

Arroyo, M., López-Manchado, M., & Herrero, B. (2003). Organo-montmorillonite as substitute of carbon black in natural rubber compounds. *Polymer, 44*(8), 2447–2453

Chen, Y., Wei, W., Zhu, Y., Luo, J., & Liu, X. (2019). Non-covalent functionalization of carbon nanotubes via co-deposition of tannic acid and polyethyleneimine for reinforcement and conductivity improvement in epoxy composite. *Composites Science and Technology, 170*(JAN.20), 25–33

Devi, K. U., Ponnamma, D., Causin, V., Maria, H. J., & Thomas, S. (2015). Enhanced morphology and mechanical characteristics of clay/styrene butadiene rubber nanocomposites. *Applied Clay Science, 114*, 568–576

de Oliveira, A. D., & Beatrice, C. A. G. (2018). Polymer nanocomposites with different types of nanofiller. *Nanocomposites – Recent Evolutions*, 103–104

Dubois, P., & Alexandre, M. (2000). Polymer-layered silicate nanocomposites: Preparation, properties and uses of a new class of materials. *Materials Science & Engineering : r: Reports, 28*(1–2), 1–63

Esmaeili, E., Rounaghi, S. A., & Eckert, J. (2021). Mechanochemical synthesis of rosin-modified montmorillonite: A breakthrough approach to the next generation of OMMT/Rubber nanocomposites. *Nanomaterials, 11*(8), 1974

Essawy, H., & El-Nashar, D. (2004). The use of montmorillonite as a reinforcing and compatibilizing filler for NBR/SBR rubber blend. *Polymer Testing, 23*(7), 803–807

Hrachová, J., Komadel, P., & Chodák, I. (2008). Effect of montmorillonite modification on mechanical properties of vulcanized natural rubber composites. *Journal of Materials Science, 43*(6), 2012–2017

Hu, J., Tian, X., Sun, J., Yuan, J., & Yuan, Y. (2020). Chitin nanocrystals reticulated self-assembled architecture reinforces deproteinized natural rubber latex film. *Journal of Applied Polymer Science, 137*(39), 49173

Jiang, G., Song, S., Zhai, Y., Chi, F., & Yong, Z. (2015). Improving the Filler Dispersion of Polychloroprene/Carboxylated Multi-walled Carbon Nanotubes Composites by Non-covalent Functionalization of Carboxylated Ionic Liquid. *Composites Science and Technology, 123*, 171–178

Joly, S., Garnaud, G., Ollitrault, R., Bokobza, L., & Mark, J. E. (2002). Organically Modified Layered Silicates as Reinforcing Fillers for Natural Rubber. *Chemistry of Materials, 14*(10), 4202–4208

Kader, M. A., Kim, K., Lee, Y. S., & Nah, C. (2006). Preparation and properties of nitrile rubber/montmorillonite nanocomposites via latex blending. *Journal of Materials Science, 41*(22), 7341–7352

Khalid, M., Walvekar, R., Ketabchi, M. R., Siddiqui, H., & Hoque, M. E. (2016). Rubber/nanoclay composites: towards advanced functional materials. *Nanoclay Reinforced Polymer Composites: Nanocomposites and Bionanocomposites*, 209–224

Nielsen, G. D., Wolkoff, P., & Alarie, Y. (2007). Sensory irritation: Risk assessment approaches. *Regulatory Toxicology and Pharmacology, 48*(1), 6–18

Rajaraman, R., Amarendra, G., Ponnamma, D, Thomas S, Varughese KT. (2015). Free-volume correlation with mechanical and dielectric properties of natural rubber/multi walled carbon nanotubes composites. *Composites Part A: Applied Science and Manufacturing, 77*, 164-171

Ravindren, R., Mondal, S., Nath, K., & Das, N. C. (2018). Investigation of electrical conductivity and electromagnetic interference shielding effectiveness of preferentially distributed conductive filler in highly flexible polymer blends nanocomposites. *Composites Part a: Applied Science and Manufacturing, 118*, 75–89

Ren, X., Barrera, C. S., Tardiff, J. L., Gil, A., & Cornish, K. (2020). Liquid guayule natural rubber, a renewable and crosslinkable processing aid in natural and synthetic rubber compounds. *Journal of Cleaner Production, 276*, 122933

Riddick, T. M. (1968). Control of colloid stability through zeta potential (Vol. 1). Wynnewood, PA: Livingston

Song, P., Xu, Z., Wu, Y., Cheng, Q., Guo, Q., & Wang, H. (2017). Super-tough artificial nacre based on graphene oxide via synergistic interface interactions of π-π stacking and hydrogen bonding. *Carbon, 111*, 807–812

Sui, G., Zhong, W. H., Yang, X. P., & Yu, Y. H. (2008). Curing kinetics and mechanical behavior of natural rubber reinforced with pretreated carbon nanotubes. *Materials Science and Engineering A, 485*(1–2), 524–531

Tang, S., Li, J., Wang, R., Zhang, J., Lu, Y., Hu, G. H., Wang, Z., & Zhang, L. (2022). Current trends in bio-based elastomer materials. *SusMat, 2*(1), 2–33

Valadares, L., & F., Leite, C., A., Galembeck, & F. (2006). Preparation of natural rubber-montmorillonite nanocomposite in aqueous medium: Evidence for polymer-platelet adhesion. *Polymer, 47*(2), 672–678

Zhang, L., Li, Y., & Xu, H. (2005). New fabricate of styrene–butadiene rubber/montmorillonite nanocomposites by anionic polymerization. *Polymer, 46*(1), 129–136